MOLECULAR AND CELLULAR BIOLOGY, June 2006, p. 4564–4576 Vol. 26, No. 12
0270-7306/06/$08.00+0 doi:10.1128/MCB.00266-06

p18^{Ink4c} and *Pten* Constrain a Positive Regulatory Loop between Cell Growth and Cell Cycle Control

Feng Bai,[1]† Xin-Hai Pei,[1]† Pier Paolo Pandolfi,[2] and Yue Xiong[1]*

Lineberger Comprehensive Cancer Center, Department of Biochemistry and Biophysics, University of North Carolina at Chapel Hill, Chapel Hill, North Carolina 27599-7295,[1] and Department of Pathology, Memorial Sloan-Kettering Cancer Center, New York, New York[2]

Received 13 February 2006/Returned for modification 15 March 2006/Accepted 26 March 2006

Inactivation of the Rb-mediated G_1 control pathway is a common event found in many types of human tumors. To test how the Rb pathway interacts with other pathways in tumor suppression, we characterized mice with mutations in both the cyclin-dependent kinase (CDK) inhibitor p18^{Ink4c} and the lipid phosphatase *Pten*, which regulates cell growth. The double mutant mice develop a wider spectrum of tumors, including prostate cancer in the anterior and dorsolateral lobes, with nearly complete penetrance and at an accelerated rate. The remaining wild-type allele of *Pten* was lost at a high frequency in *Pten*$^{+/-}$ cells but not in *p18*$^{+/-}$ *Pten*$^{+/-}$ or *p18*$^{-/-}$ *Pten*$^{+/-}$ prostate tumor cells, nor in other *Pten*$^{+/-}$ tumor cells, suggesting a tissue- and genetic background-dependent haploinsufficiency of *Pten* in tumor suppression. *p18* deletion, CDK4 overexpression, or oncoviral inactivation of Rb family proteins caused activation of Akt/PKB that was recessive to the reduction of PTEN activity. We suggest that *p18* and *Pten* cooperate in tumor suppression by constraining a positive regulatory loop between cell growth and cell cycle control pathways.

Genetic and pathological analyses of both human populations and transgenic animal models have established that tumorigenesis is a multistep process involving alteration of both proto-oncogenes and tumor suppressor genes in a single individual tumor cell. Functional collaborations between gain-of-function mutations of activated oncogenes and between loss-of-function mutations targeting tumor suppressor genes are common events required for the progressive evolution of a normal cell into a cancerous one (13). One of several well-characterized tumor suppression pathways is the Rb pathway, which includes three related proteins in mammalian cells, pRb, p107, and p130, that play critical roles collaboratively in controlling mammalian G_1 cell cycle progression (32). Emerging from mitosis or present in quiescent cells as hypophosphorylated forms, these proteins negatively regulate the activity of E2F transcription factors to prevent S-phase entry. Extracellular mitogens induce the expression of D-type cyclins and activate cyclin D-dependent kinases CDK4 and CDK6, leading to phosphorylation and functional inactivation of Rb proteins. Conversely, inhibition of CDK4 and CDK6, resulting from either lack of cyclin D synthesis or binding with an INK4 protein, retains Rb proteins in their growth-suppressive states and prevents the G_1-to-S transition. Disruption of this pathway, consisting of INK4-cyclin D/CDK4/6-Rb-E2F, deregulates G_1 cell cycle progression and is a common event for the development of most types of cancer (28). Genetic study in targeted mice provides strong support for a critical function of this pathway in tumor suppression. Mice develop spontaneous tumors when they are heterozygous for *Rb* (14, 21), chimeric for *Rb*$^{-/-}$ (22, 33), deficient for CDK inhibitors p18^{Ink4c} (11, 12, 20) and p16^{Ink4a} (18, 27), or carrying an INK4-insensitive mutation (R24C) in *CDK4* (29).

A persistent puzzle from the studies of mice with germ line mutations impairing the Rb pathway is why tumors that develop in these mice exhibit a spectrum different from that observed in human patients. While heterozygosity of the *Rb* gene is causally linked with the development of retinoblastoma (17), mice heterozygous for *Rb* or chimeric for *Rb*$^{-/-}$ developed tumors almost exclusively in neuroendocrine organs, including the characteristic intermediate lobe of the pituitary and four additional endocrine organs: the thyroid, parathyroid, adrenal glands, and pancreatic islets. Moreover, germ line mutations in mice that targeted the upstream activators of Rb, the CDK inhibitor genes, resulted in the development of neuroendocrine tumors with a very similar spectrum: single *p18*$^{-/-}$ and *p27*$^{-/-}$ deficient mice develop slow-growing intermediate lobe pituitary tumors (11), and the *p18 p27* double mutant mice, either three-fourths or double null, develop tumors with a complete or high penetrance in the same endocrine cells as in *Rb* mutant mice by the age of 4 months (12). The bases of the tissue specificity of tumor development and of the species difference caused by the germ line mutations targeting the Rb pathway are not known. One explanation of the tissue specificity of tumors developed in mice with reduced function of the Rb pathway is that the functional collaboration between the Rb and other pathways controlling different cellular processes may determine the spectrum of tumor specificity. To test how tumor suppressor genes acting on different pathways collaborate with each other to suppress tumor development, we set out to characterize mice with compound mutations in *p18* and *Pten*.

The *PTEN* (*p*hosphatase and *ten*sin homolog deleted from chromosome 10, also known as MMAC1 or TEP1) tumor suppressor is located on a genomic region that frequently suf-

* Corresponding author. Mailing address: Lineberger Comprehensive Cancer Center, Department of Biochemistry and Biophysics, University of North Carolina at Chapel Hill, Chapel Hill, NC 27599-7295. Phone: (919) 962-2142. Fax: (919) 966-8799. E-mail: yxiong@email.unc.edu.

† F.B. and X.-H.P. contributed equally to this work.

fers loss of heterozygosity (LOH) in different types of advanced human cancer, including prostate cancer (4). Genetic analysis of *Pten* mutant mice sustaining monoallelic or null mutations supports a key function of PTEN in suppressing prostate tumor development (7, 9, 25, 30, 31). The biochemical mechanism underlying PTEN′s tumor suppression function is believed to lie in its phosphatase activity. Most missense mutations in *Pten* detected in primary tumors and in established cell lines are confined to exon 5, encoding the phosphatase domain. The main in vivo substrate of PTEN phosphatase activity is the lipid second messenger, phosphatidylinositol 3,4,5-triphosphate (23), placing PTEN into a previously defined signaling pathway in which the proto-oncogene serine/threonine kinase Akt is a major effector of PTEN. The cellular function of PTEN was recently linked to cell growth control by the findings that TSC1/2, a heterodimeric complex consisting of TSC1 and TSC2 whose mutations predispose individuals to hamartomas in many tissues and inhibit mTOR-mediated protein synthesis, is a major downstream target of AKT (3). We reasoned that simultaneous stimulation of cell growth, resulting from a reduction of PTEN activity, and the cell cycle, caused by the loss of function of p18, may more effectively promote tumor development than the alteration of either pathway alone. We report in this paper the characterization of tumor development in *p18-Pten* double mutant mice.

MATERIALS AND METHODS

Mice. The generation and genotyping of *p18* and *Pten* mutant mice have been described previously (8, 11). *p18* and *Pten* mutant mice have been backcrossed for 9 and more than 15 generations with C57BL/6 mice, respectively. Cohorts were housed and analyzed in a common setting, and littermate controls were used for all experiments as indicated.

Histopathology, immunological procedures, and antibodies. Tissues were fixed and examined by two pathologists after hematoxylin-eosin staining. Immunohistochemistry was performed as described previously (2). To measure proliferating and mitotic cells, sections were blocked with normal goat serum in phosphate-buffered saline and incubated with the antibody against phospho-histone H3 (5 $\mu g\ ml^{-1}$) followed by biotin-conjugated secondary antibody. Immunocomplexes were detected using the Vectastain ABC alkaline phosphatase kit. Terminal deoxynucleotidyltransferase-mediated dUTP biotin nick end labeling (TUNEL) assays were carried out using an in situ ApopTag kit (Intergen) according to the manufacturer's protocol. Antibodies to phospho-Akt^{Ser473}, calcitonin (Research Diagnostics), B220, CD3 (BD Pharmingen), Akt, phospho-S6K^{Thr389} (Cell Signaling Technology), myc (9E10), simian virus 40 large T (Oncogene), phospho-histone H3 ser10 (Upstate Biotechnology), and actin (Santa Cruz Biotechnology, Inc.) were purchased commercially.

Laser capture microdissection and LOH analysis. Laser capture microdissection was used to obtain pure cell populations of selected areas from paraffin-embedded tissue sections. Ten-micrometer sections were deparaffinized and lightly stained with hematoxylin. Using a PixCell lle laser capture microdissection system (Arcturus, Mountain View, CA), the lesions that were clearly separated from normal tissues were isolated from the slides. DNA was isolated from the microdissected tissue samples as described before.

Cell culture, treatment, and transfection. LNCaP and DU145 cells were cultured in RPMI 1640 medium with 10% fetal bovine serum. Cells were transfected with FuGene. Where indicated, 20 μM LY294002 or dimethyl sulfoxide solvent was added to the cells 24 h prior to lysis.

Statistical analyses. All of the statistical analyses were performed with the program StatsDirect 2.4.3 (StatsDirect Statistical Software). The survival rate was calculated by the Kaplan-Meier method. Fisher's exact test was used to test for the difference in the probability of developing tumors between mice with compound deletions and those with single gene deletions.

RESULTS

Accelerated tumorigenesis in *p18 Pten* double mutant mice. To test the genetic interaction between *p18* and *Pten*, we mated $p18^{-/-}$ homozygotes with $Pten^{+/-}$ heterozygotes, both from a C57BL/6 background, to generate animals heterozygous for both genes. These mice were intercrossed to generate both $p18^{-/-}$ $Pten^{+/-}$ and $p18^{+/-}$ $Pten^{+/-}$ animals. Genotype analysis of more than 200 offspring did not identify any $p18^{-/-}$ $Pten^{-/-}$ double null mice, nor were any viable $p18^{-/-}$ $Pten^{-/-}$ embryos identified beyond embryonic day 7.5 (data not shown). These results indicate that deletion of *p18* does not rescue the embryonic lethality caused by *Pten* loss.

A cohort of 54 $p18^{-/-}$ $Pten^{+/-}$ and 32 $p18^{+/-}$ $Pten^{+/-}$ mice was monitored for their development and survival along with $p18^{-/-}$ ($n = 46$), $Pten^{+/-}$ ($n = 35$), and wild-type mice ($n = 30$) (Fig. 1a). Both $p18^{-/-}$ $Pten^{+/-}$ and $p18^{+/-}$ $Pten^{+/-}$ mice undergo normal development overall into their adulthood, and no significant developmental defects were detected. However, both mice had a decreased life span compared to either $Pten^{+/-}$ or $p18^{-/-}$ mice. Whereas most $p18^{-/-}$ mice lived beyond 500 days and the mean age at death of $Pten^{+/-}$ mice was 303 days, the mean ages at death of $p18^{+/-}$ $Pten^{+/-}$ and $p18^{-/-}$ $Pten^{+/-}$ mice were 245 and 187 days, respectively, which was significantly lower than $Pten^{+/-}$ or $p18^{-/-}$ alone mice (Fig. 1a). The direct cause of earlier death of these double mutant mice, as in the case for $Pten^{+/-}$ mice (8), is likely the kidney failure caused by autoimmune glomerulopathy, which was accelerated by the *p18* loss. $Pten^{+/-}$ mice, beginning at 3 months of age, developed lymphadenopathy affecting mainly the submandibular and axillary lymph nodes. By the age of 6 months, most lymph nodes were between 0.5 and 1.5 cm in size, and the average size was 0.96 ± 0.45 cm (mean $\pm$ standard deviation) in diameter (Fig. 1b and c). The development of lymphadenopathy was accelerated by *p18* loss; all $p18^{-/-}$ $Pten^{+/-}$ double mutant mice developed lymphadenopathy at the age of 3 months. Most lymph nodes were larger than 1.5 cm, and the average size was 2.1 ± 0.71 cm by the age of 6 months in these double mutant mice (Table 1; Fig. 1c). Severe autoimmune glomerulopathy became evident as early as 3 months of age in the $p18^{-/-}$ $Pten^{+/-}$ mice, which might have contributed to the renal failure associated with the early death of $p18^{-/-}$ $Pten^{+/-}$ mice. The lymphocytes from enlarged lymph nodes and spleens from both $Pten^{+/-}$ and $p18^{-/-}$ $Pten^{+/-}$ mice were polyclonal, as verified by staining of the T-cell marker CD3 and the B-cell marker B220 with immunohistochemistry (IHC) and flow cytometric analysis (data not shown).

The *p18 Pten* double mutant mice developed tumors at an accelerated rate with a wider spectrum than either single mutant. As a brief overview, 74% ($n = 19$) of $p18^{-/-}$ $Pten^{+/-}$ double mutant mice developed pituitary tumors in both anterior and intermediate lobes by the age of 10 months, whereas none of the $p18^{-/-}$ or $Pten^{+/-}$ single mutant mice developed tumors in both lobes (Fig. 2). Pheochromocytomas developed in the adrenals of 84% of $p18^{-/-}$ $Pten^{+/-}$ mice, compared to 65% in $Pten^{+/-}$ and 14% in $p18^{-/-}$ mice, and these were more aggressive, compressing the adrenal cortex, exhibiting more mitotic figures, and frequently invading into the cortex and surrounding tissues (Fig. 3). C-cell tumors developed in 63%

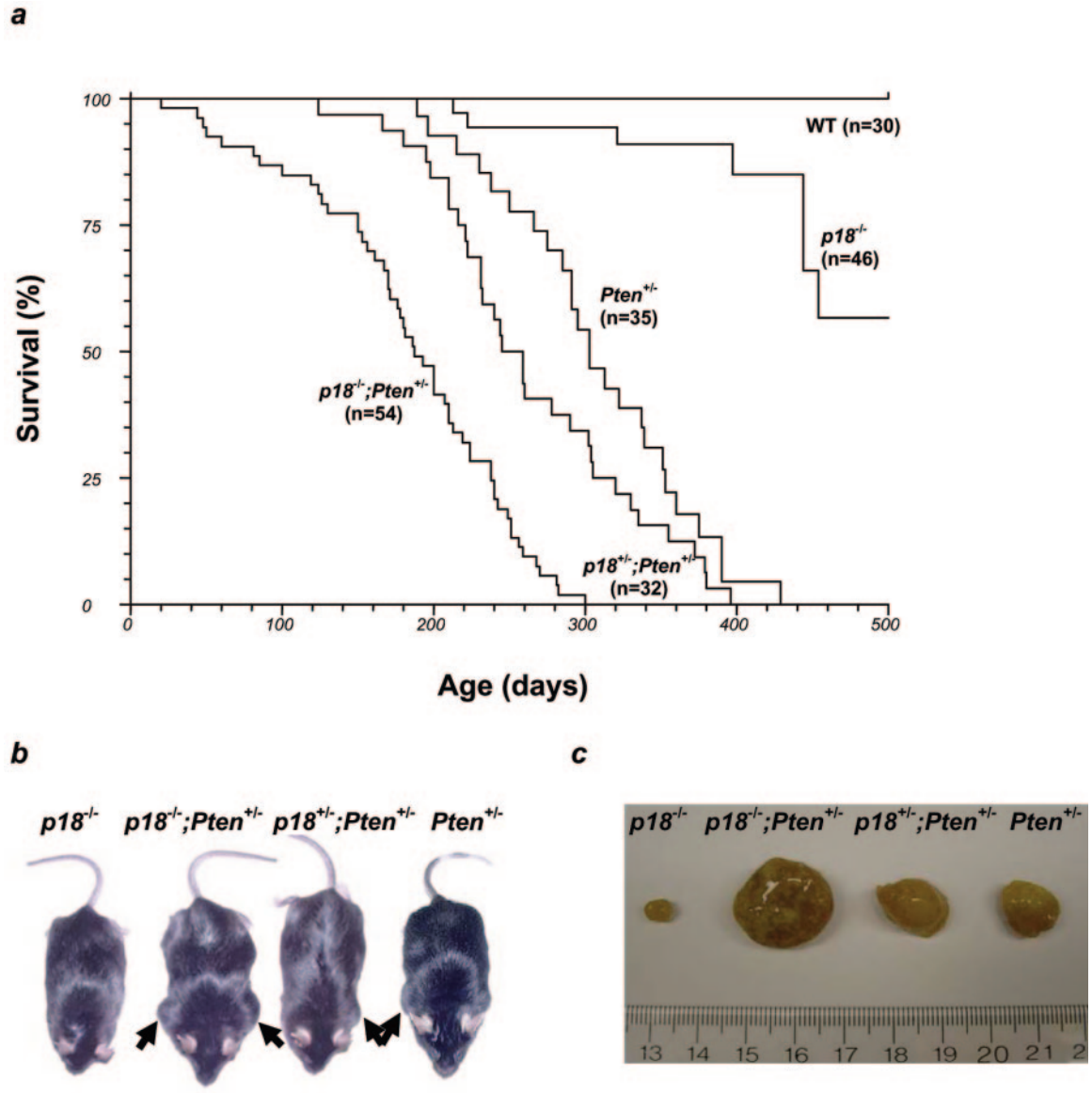

FIG. 1. Survival and lymphadenopathy of *p18* and *Pten* mice. (a) The graph summarizes the viability of mice with each genotype. The mean age of survival is given in Results. (b) Mice of different genotypes of the same litter at 6 months of age. Enlarged lymph nodes are indicated. (c) Gross appearance of lymph nodes from different mice at 6 months of age.

($n = 19$) of $p18^{-/-}$ $Pten^{+/-}$ mice, compared with only 14% ($n = 14$) and 15% ($n = 20$) of $p18^{-/-}$ and $Pten^{+/-}$ mice, respectively. Moreover, half of the $p18^{-/-}$ $Pten^{+/-}$ mice developed thyroid tumors of both C cells and follicular cells, but only 15% of $Pten^{+/-}$ mice and no $p18^{-/-}$ mice developed thyroid tumors in both cell types (Table 1; Fig. 3). At 6 months of age, 80% of $p18^{-/-}$ $Pten^{+/-}$ mice displayed high-grade prostatic intraepithelial neoplasia (PIN) in both the anterior and dorsolateral prostatic lobes, including 20% invasive tumors, compared with only one in eight (13%) $Pten^{+/-}$ mice and no $p18^{-/-}$ mice developing high-grade PIN. Late in life (>12 months), all $p18^{+/-}$ $Pten^{+/-}$ mice, as opposed to half of the $Pten^{+/-}$ and none of the $p18^{-/-}$ mice, developed high-grade PIN (Fig. 4). Nearly every $p18^{-/-}$ $Pten^{+/-}$ mouse developed multiple tumors in different organs. These results offer a glimpse of the data that support a functional collaboration between *p18* and *Pten* in suppression of tumorigenesis.

***p18*$^{-/-}$ *Pten*$^{+/-}$ mice developed pituitary tumors in both the anterior and intermediate lobes.** Consistent with previous reports (11, 12), more than half of the $p18^{-/-}$ mice developed pituitary intermediate lobe tumors between 6 and 16 months of age. Thirty-five percent of $Pten^{+/-}$ mice also developed pituitary tumors between 6 and 14 months of age, a phenotype that has not been previously reported. Unlike the characteristic intermediate lobe tumors that developed in mice with reduced or disrupted function of genes acting on the Rb pathway, all the pituitary tumors that arose in $Pten^{+/-}$ mice were located in the anterior lobe (Fig. 2). Loss of one *p18* allele did not significantly increase the incidence of anterior lobe tumors in $Pten^{+/-}$ mice, but *p18* nullizygosity shortened the latency of

TABLE 1. Spontaneous tumor formation and incidence in $p18^{-/-}$, $Pten^{+/-}$, $p18^{+/-}$ $Pten^{+/-}$, and $p18^{-/-}$ $Pten^{+/-}$ mice

Organ and/or condition	No. (%) animals with tumor								
	Wild type 10–14 mos (n = 15)	$p18^{-/-}$		$Pten^{+/-}$		$p18^{+/-}$ $Pten^{+/-}$		$p18^{-/-}$ $Pten^{+/-}$	
		3–6 mos (n = 6)	6–16 mos (n = 14)	3–6 mos (n = 9)	6–14 mos (n = 20)	3–6 mos (n = 8)	6–13 mos (n = 17)	3–6 mos (n = 8)	6–10 mos (n = 19)
Pituitary									
Normal	15	6	6	9	13	8	8	6	3
Intermediate lobe tumor	0	0	8 (57)[b]	0	0	0	0	2 (25)	16 (84)
Anterior lobe tumor	0	0	0	0	7 (35)[c]	0	9 (53)[d]	1 (13)	14 (74)
Both	0	0	0	0	0	0	0	1 (13)	14 (74)
Adrenal									
Normal	14	6	8	3	5	4	4	3	1
Medullary hyperplasia	1	0	4	4	2	2	1	1	2
Pheochromocytoma	0	0	2 (14)[e]	2 (22)	13 (65)[f]	2 (25)	12 (71)[g]	4 (50)	16 (84)
Cortical adenoma	0	0	0	0	0	0	0	0	2 (11)
Thyroid									
Normal	15	6	12	8	7	7	3	4	1
C-cell tumor	0	0	2 (14)[h]	0	3 (15)[i]	0	3 (18)[k]	3 (38)	12 (63)
Follicular cell tumor	0	0	0	1 (11)	13 (65)[j]	1 (13)	13 (77)[l]	4 (50)	16 (84)
Both	0	0	0	0	3 (15)	0	2 (12)	3 (38)	10 (53)
Other tumors									
Lung	0		0		2		0		2
Breast	0		0		2		1		3
Endometrial hyperplasia	0		0		3		1		2
Harderian gland	0		1		0		0		0
Harderian gland	0		1		0		0		0
Lymphadenopathy	−		−		+		+/++		+++

[a] +, at the age of 6 months the average size of the lymph node was 0.96 ± 0.45 cm; ++, most lymph nodes were 1 to 2 cm; +++, average lymph node size was 2.1 ± 0.71 cm.
[b] $P = 0.0047$ for $p18^{-/-}$ versus $p18^{-/-}$ $Pten^{+/-}$.
[c] $P = 0.001$ for $Pten^{+/-}$ versus $p18^{-/-}$ $Pten^{+/-}$.
[d] $P = 0.11$ for $p18^{+/-}$ $Pten^{+/-}$ versus $p18^{-/-}$ $Pten^{+/-}$.
[e] $P < 0.001$ for $p18^{-/-}$ versus $p18^{-/-}$ $Pten^{+/-}$; $P = 0.0012$ for $p18^{-/-}$ versus $p18^{+/-}$ $Pten^{+/-}$.
[f] $P = 0.098$ for $Pten^{+/-}$ versus $p18^{-/-}$ $Pten^{+/-}$; $P = 0.36$ for $Pten^{+/-}$ versus $p18^{+/-}$ $Pten^{+/-}$.
[g] $P = 0.18$ for $p18^{+/-}$ $Pten^{+/-}$ versus $p18^{-/-}$ $Pten^{+/-}$.
[h] $P = 0.003$ for $p18^{-/-}$ versus $p18^{-/-}$ $Pten^{+/-}$.
[i] $P = 0.0014$ for $Pten^{+/-}$ versus $p18^{-/-}$ $Pten^{+/-}$.
[j] $P = 0.098$ for $Pten^{+/-}$ versus $p18^{-/-}$ $Pten^{+/-}$.
[k] $P = 0.004$ for $p18^{+/-}$ $Pten^{+/-}$ versus $p18^{-/-}$ $Pten^{+/-}$.
[l] $P = 0.2$ for $p18^{+/-}$ $Pten^{+/-}$ versus $p18^{-/-}$ $Pten^{+/-}$.

anterior lobe tumors from 11.5 ± 3 months in $Pten^{+/-}$ mice to 7.5 ± 2 months in $p18^{-/-}$ $Pten^{+/-}$ mice and increased the incidence of anterior lobe tumors from 35% in $Pten^{+/-}$ mice to 74% in $p18^{-/-}$ $Pten^{+/-}$ mice (Table 1). Although $Pten^{+/-}$ mice did not develop obvious pathological abnormalities in the intermediate lobe, the incidence of intermediate lobe tumors was increased from 57% in $p18^{-/-}$ mice to 84% in $p18^{-/-}$ $Pten^{+/-}$ (Table 1 and Fig. 2).

To confirm the functional collaboration between *p18* and *Pten* in suppressing pituitary tumor development in both lobes, we carried out more detailed histological analyses of mice of different genotypes at both an early age (3 to 6 months) (Fig. 2a) and late in life (after 6 months) (Fig. 2b). At the early age, both $p18^{-/-}$ single mutant and $p18^{+/-}$ $Pten^{+/-}$ double heterozygous mice developed hyperplasia in the intermediate lobe, while nearly all $Pten^{+/-}$ pituitaries were normal. At this age, 25% of $p18^{-/-}$ $Pten^{+/-}$ mice had already developed adenomas in the intermediate lobe and, notably, one out of eight mice also developed an adenoma in the anterior lobe, a phenotype that was not visible in $p18^{-/-}$, $p18^{+/-}$ $Pten^{+/-}$, or $Pten^{+/-}$ mutant mice at this age. Late in life, 5 of 20 (25%) and 2 of 20 (10%) $Pten^{+/-}$ mice developed adenoma and adenocarcinoma, respectively, exclusively in the anterior lobe (Fig. 2b). Eight of 14 (57%) $p18^{-/-}$ mice developed intermediate lobe adenoma and adenocarcinoma. Remarkably, 14 of 19 (74%) of $p18^{-/-}$ $Pten^{+/-}$ mice developed adenoma and adenocarcinoma in both anterior and intermediate lobes. The tumors in the $p18^{-/-}$ $Pten^{+/-}$ mice were more aggressive and severe; hemorrhaging, necrosis, and invasion into adjacent tissues were evident (Fig. 2b). Immunostaining of serial pituitary sections with antibodies to mitotic phosphorylated histone H3 revealed an increase of cell proliferation in the $p18^{+/-}$ $Pten^{+/-}$ pituitary and an even higher level of proliferation in $p18^{-/-}$ $Pten^{+/-}$ cells than either $p18^{-/-}$ or $Pten^{+/-}$ pituitaries (Fig. 2c), indicating that *Pten*, like *p18*, also plays a role in restraining cell proliferation.

Loss of both *p18* and *p27* resulted in spontaneous development of hyperplastic tissues and/or tumors in the pituitary, adrenals, thyroid, parathyroid, testis, and pancreas (12), a phenotype that is similar to human multiple endocrine neoplasia

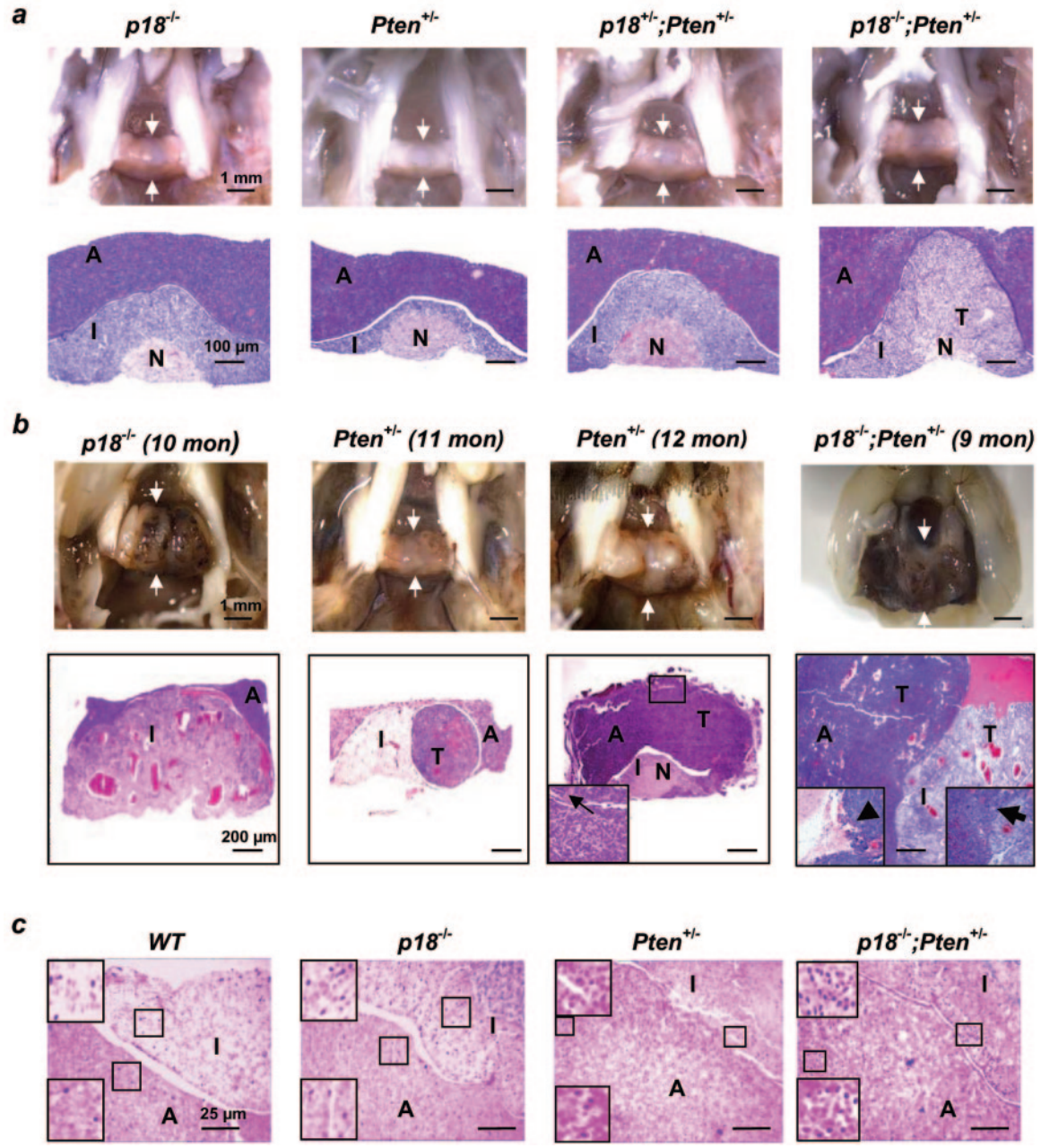

FIG. 2. Collaboration between *Pten* and *p18* in suppression of pituitary tumors. (a) Pituitary glands (arrows) from different genotypes of mice of the same litter were microscopically examined at 3.5 months of age either directly (top row) or after hematoxylin and eosin staining (bottom row). Anterior lobe (A), intermediate lobe (I), neurohypophysis (N), and a tumor (T) are indicated. (b) Pituitary tumorigenesis in different genotypes of mice late in life (after 9 months). The boxed area in the $Pten^{+/-}$ image is magnified in the inset. The arrow indicates the area of invasion from the anterior lobe into surrounding bone tissue. The lower right inset for $p18^{-/-}$ $Pten^{+/-}$ shows the area of invasion from the intermediate lobe into the anterior lobe (arrow). The lower left inset for $p18^{-/-}$ $Pten^{+/-}$ shows the anterior lobe tumor invading into the surrounding brain tissue (arrowhead). (c) Series of sections of pituitary glands from mice of different genotypes at 9 months of age were examined for mitotic activity by immunostaining with an antibody recognizing phosphorylated histone H3. Boxed areas are magnified in the insets (anterior lobe [lower left] and intermediate lobe [upper left]).

(MEN) syndromes and implicates *p18* and *p27* as MEN genes. One puzzling difference between the clinical manifestation of human MEN syndromes and the phenotypes that developed in $p18^{-/-}$ $p27^{-/-}$ mice is that while MEN patients develop pituitary tumors in the anterior lobe, nearly all pituitary tumors that developed in $p18^{-/-}$ $p27^{-/-}$ mice were from the intermediate lobe. Identification of a *p18* function in the anterior lobe provides further support for a role of *p18* in suppression of MEN.

Twenty to 25% of humans develop pituitary adenomas, as revealed by autopsy, and nearly all lesions develop in the anterior lobe, not the intermediate lobe (10). The prevalence of

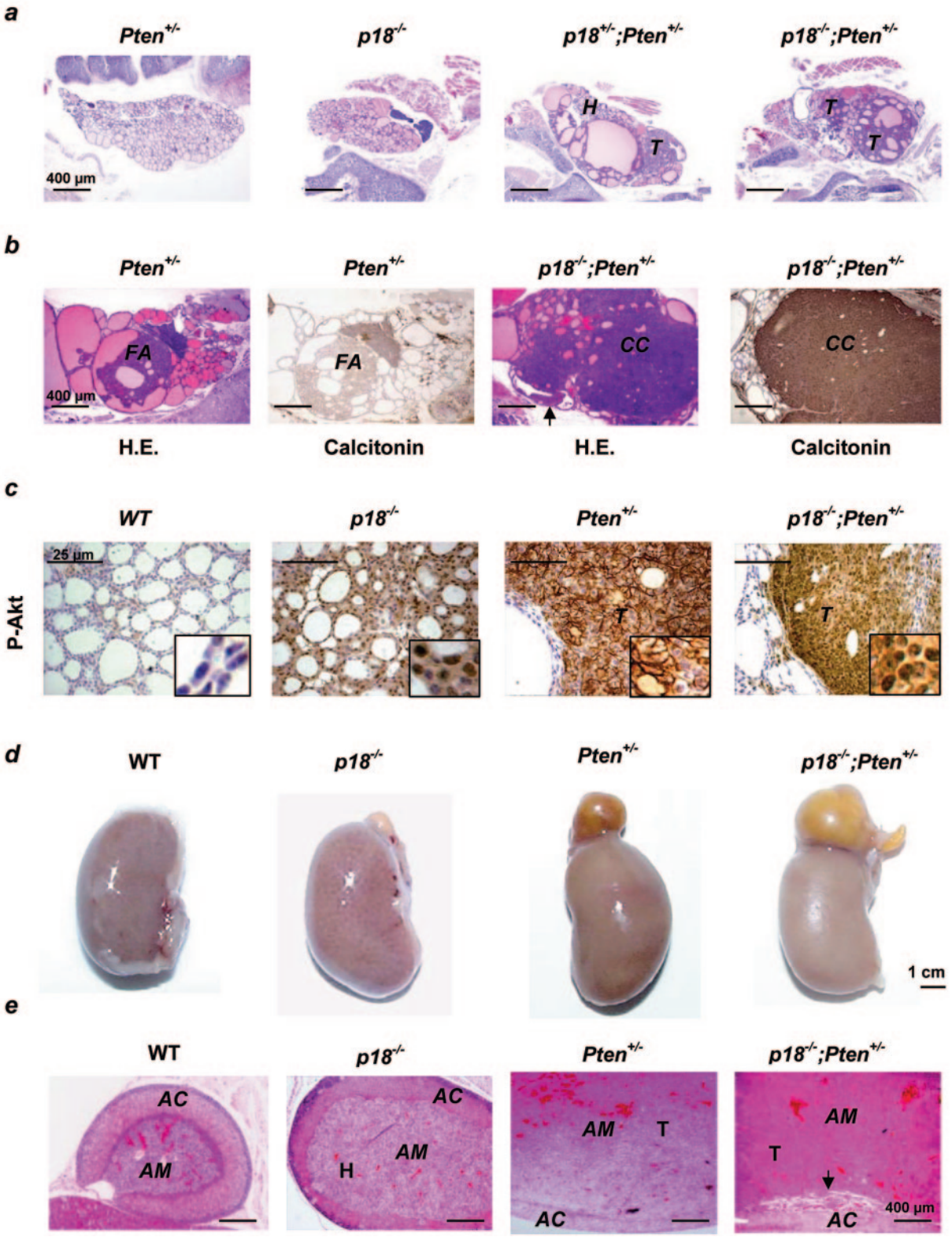

FIG. 3. Collaboration between *Pten* and *p18* in suppression of thyroid and adrenal tumors. (a) Hematoxylin and eosin staining of thyroids from mice of different genotypes at 3 months of age. Hyperplasia (H) and tumor (T) are indicated. (b) Thyroid tumors from mice of the same litter were examined at 9 months of age by hematoxylin and eosin staining and by immunostaining for calcitonin. Follicular cell adenoma (FA) and C-cell carcinoma (CC) are indicated. Calcitonin-containing tumor cell invasion is indicated by an arrow. (c) Immunostaining of the thyroid from wild-type (WT) and $p18^{-/-}$ mice (12 months of age) and of C-cell tumors from $Pten^{+/-}$ (12 months of age) and $p18^{-/-}$ $Pten^{+/-}$ (9 months of age) mice for phospho-Akt. (d) Gross appearance of adrenal glands from $Pten^{+/-}$ (10 months of age), $p18^{-/-}$ $Pten^{+/-}$ (9 months), and WT and $p18^{-/-}$ (13 months) mice. (e) Hematoxylin and eosin staining of adrenal glands from different genotypes. Hyperplasia (H) and pheochromocytoma (T) of the adrenal medulla (AM) compressing the adrenal cortex (AC) are indicated. The arrow indicates the area of invasion from the medulla into the cortex. Note the intact medulla-cortex boundary in $Pten^{+/-}$ mice and disruption of the boundary in $p18^{-/-}$ $Pten^{+/-}$ mice.

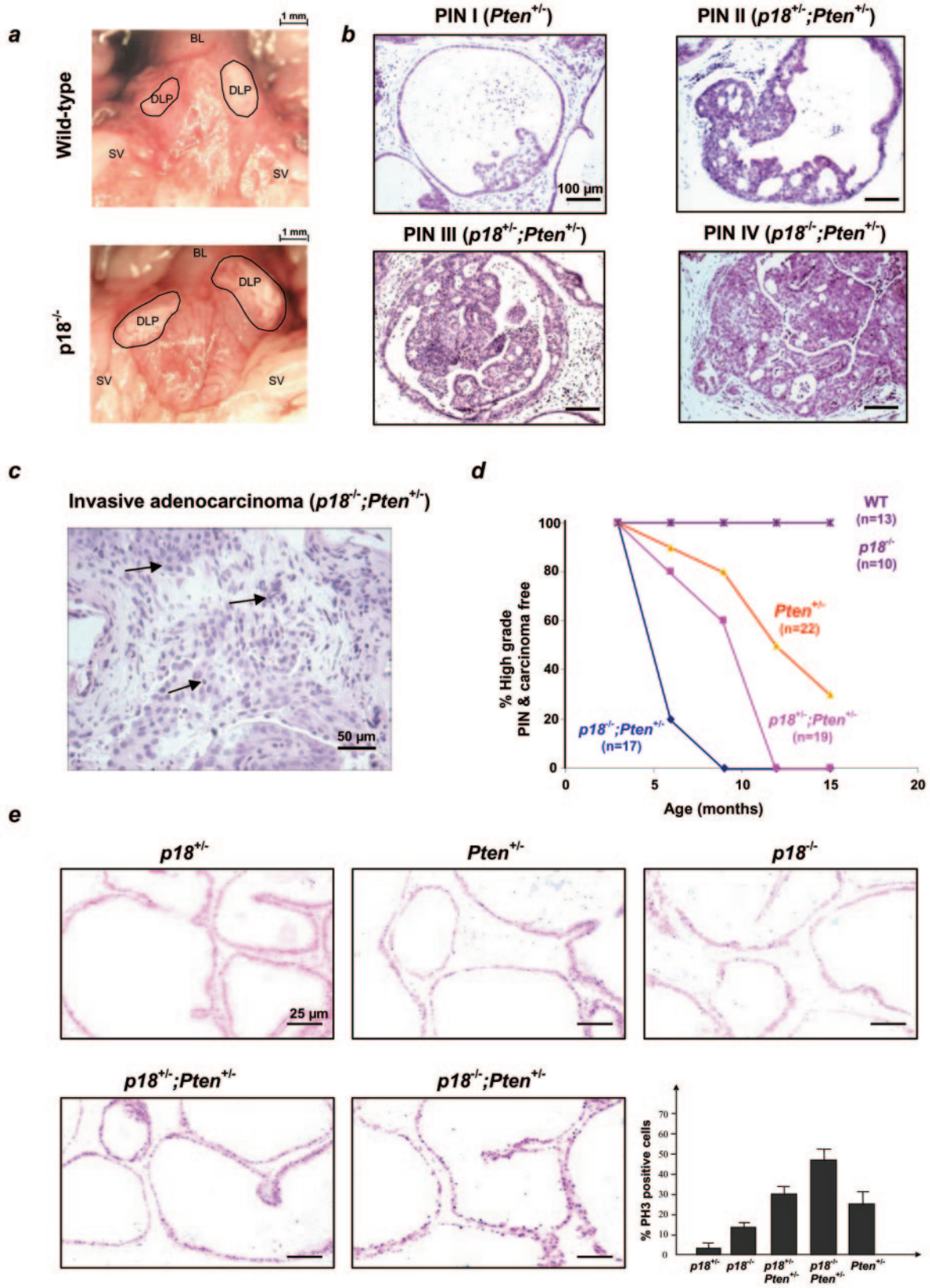

FIG. 4. *p18* and *Pten* cooperate in prostate tumor suppression. (a) Gross appearances of age-matched wild-type (WT) and $p18^{-/-}$ mice (12 months) are shown. Significant enlargement of the dorsolateral prostate (DLP) was seen. SV, seminal vesicle; BL, bladder. (b) Representative hematoxylin and eosin staining of prostates from mice of different genotypes at 6 months of age. Diagnostic criteria for PIN are described in the text. (c) Representative invasive adenocarcinoma from $p18^{-/-}$ $Pten^{+/-}$ prostates at 9.5 months of age. Nests of tumor cells invading into the stroma

these tumors has long been underestimated because of their small size and noninvasive nature. Although the mortality rate is low, pituitary adenomas cause various symptoms, such as inappropriate hormone secretion, headaches, and deterioration of visual acuity. These results thus also suggest the p18-CDK4-Rb pathway as a potential target for therapeutic intervention of both MEN and pituitary adenoma.

Accelerated thyroid tumorigenesis in *p18*$^{-/-}$ *Pten*$^{+/-}$ mice. Thyroid tissues contain large follicles surrounded by follicular cells and scattered C cells. Consistent with a previous report (7), we detected follicular cell tumors in 14 out of 29 (48%) *Pten*$^{+/-}$ mice and C-cell tumors at a much lower incidence (3 out of 29) (Fig. 3a). Two out of 20 *p18* null mice developed thyroid tumors, all of which were C-cell tumors (Table 1). The C-cell origin of these tumors was verified by immunohistochemistry using an antibody to calcitonin (Fig. 3b). Most tumors derived from both *Pten*$^{+/-}$ and *p18*$^{-/-}$ mutant mice were small, confined to one lobe, and did not alter the gross appearance of the thyroid. *p18* deficiency shortened the latency and changed the spectrum of thyroid tumor development in *Pten*$^{+/-}$ mice. Between the ages of 3 and 6 months, half (four of eight) of the *p18*$^{-/-}$ *Pten*$^{+/-}$ mice had already developed follicular cell tumors, three of which were combined with C-cell tumors, while no C-cell tumors were found in *p18*$^{-/-}$ or *Pten*$^{+/-}$ mice, and only one out of nine *Pten*$^{+/-}$ mice developed a follicular cell tumor at the same age (Table 1). Late in life (>6 months), 63% of *p18*$^{-/-}$ *Pten*$^{+/-}$ mice had C-cell tumors, compared with only 14% and 15% of *p18*$^{-/-}$ and *Pten*$^{+/-}$ mice at the same age, respectively. Sixteen out of 19 (84%) of the *p18*$^{-/-}$ *Pten*$^{+/-}$ mice developed follicular cell tumors, higher than the incidences of follicular cell tumors in both *p18*$^{+/-}$ *Pten*$^{+/-}$ (77%) and *Pten*$^{+/-}$ (65%) mice (Table 1). Fifty-three percent of *p18*$^{-/-}$ *Pten*$^{+/-}$ thyroids that developed C-cell tumors also developed follicular cell tumors, either in the same lobe or the other lobe. Tumors that arose in *p18*$^{-/-}$ *Pten*$^{+/-}$ thyroids were large, obvious by gross analysis, and often bilateral, indicating increased malignancy over the tumors that arose in either *p18*$^{-/-}$ or *Pten*$^{+/-}$ thyroids at a similar age.

Immunostaining of the thyroid tumors with an antibody to Ser^{473}-phosporylated Akt revealed an increased level of activated Akt that accumulated mostly at the plasma membrane in *Pten*$^{+/-}$ thyroid C cells (Fig. 3c). Deletion of *p18* resulted in a notable increase of Ser^{473}-phosphorylated Akt in the presence of both *Pten* alleles and synergistically activated Akt in *Pten*$^{+/-}$ thyroid C cells, suggesting a negative regulation of Akt activation by *p18*.

Adrenal tumorigenesis in *p18 Pten* double mutant mice. Two out of nine (22%) *Pten*$^{+/-}$ mice and none of the *p18*$^{-/-}$ mice developed pheochromocytomas between 3 and 6 months, respectively, while late in life, 65% of *Pten*$^{+/-}$ and 14% of *p18*$^{-/-}$ mice developed pheochromocytomas (Table 1 and Fig. 3d). The tumors that occurred in either *p18*$^{-/-}$ or *Pten*$^{+/-}$ mice were generally small and occasionally invasive into the cortex, and the majority of these tumors were unilateral. On the other hand, the adrenal glands of *p18*$^{-/-}$ *Pten*$^{+/-}$ mice were clearly larger by gross examination than age-matched *p18*$^{-/-}$ or *Pten*$^{+/-}$ mice (Fig. 3d). At an early age, half of the *p18*$^{-/-}$ *Pten*$^{+/-}$ mice displayed pheochromocytoma. By the age of 10 months, most *p18*$^{-/-}$ *Pten*$^{+/-}$ mice developed pathological abnormalities in the adrenals, ranging from severe medulla hyperplasia (11%) or pheochromocytoma (84%) to pheochromocytoma combined with cortical adenoma (11%). Ten out of 16 (63%) of the *p18*$^{-/-}$ *Pten*$^{+/-}$ mice displayed bilateral pheochromocytoma, and 2 mice simultaneously developed pheochromocytoma and cortical adenoma (Table 1). The pheochromocytomas that arose in *p18*$^{-/-}$ *Pten*$^{+/-}$ mice were more aggressive than those that developed in *p18*$^{-/-}$ or *Pten*$^{+/-}$ single mutant mice; they were larger in size, compressing the adrenal cortex, exhibited more mitotic figures, and frequently invaded into the cortex and surrounding tissues (Fig. 3e). The earlier onset, increased incidence, and malignancy of adrenal tumor phenotypes in *p18*$^{-/-}$ *Pten*$^{+/-}$ mice indicate a functional collaboration between *p18* and *Pten* in suppression of adrenal tumorigenesis. These results are consistent with a model that, while both genes participate in suppression of pheochromocytoma and cortical adenoma development in the adrenal glands, *Pten* plays a more prominent role and acts at an earlier stage than *p18*.

***p18*$^{-/-}$ *Pten*$^{+/-}$ mice developed prostate tumors in the anterior and dorsolateral lobes.** *Pten*$^{+/-}$ mice are highly prone to the development of PIN (7, 25, 31). Close examination of old *p18*$^{-/-}$ male mice revealed an evident enlargement of their prostate glands, approximately 80% larger than age-matched wild-type mice (Fig. 4a). At 6 months of age, most *Pten*$^{+/-}$ prostates developed low-grade PIN (the prostatic epithelium displayed one or two layers of atypical cells), while the *p18*$^{-/-}$ prostates were normal (Fig. 4b). One out of eight *Pten*$^{+/-}$ mice developed high-grade PIN, including lesions that were large, with pleomorphic nuclei and cells filling the lumen, but the duct outline was intact, and lesions that contained atypical cells that filled the lumen and bulged focally into or invaded into surrounding tissues. An evident functional collaboration between *p18* and *Pten* in suppressing prostate tumorigenesis was seen by the increased incidence of high-grade PIN and the presence of invasive adenocarcinoma in the double mutant mice, both *p18*$^{+/-}$ *Pten*$^{+/-}$ and *p18*$^{-/-}$ *Pten*$^{+/-}$, over that in *Pten*$^{+/-}$ single mutant mice (Fig. 4b, c, and d). Four out of five (80%) *p18*$^{+/-}$ *Pten*$^{+/-}$ double heterozygotes displayed low-grade PIN with two or more layers of atypical cells, and 20% developed high-grade PIN (Fig. 4b and d). Prostate tumorigenesis was further accelerated by the loss of both *p18* alleles; 80% of *p18*$^{-/-}$ *Pten*$^{+/-}$ mice displayed high-grade PIN in both the anterior and dorsolateral prostatic lobes by 6 months of age. Twenty percent of *p18*$^{-/-}$ *Pten*$^{+/-}$ prostate tumors were microinvasive, as seen by the rupture of the basal membrane of

areas are indicated. (d) The high-grade PIN and carcinoma-free curve shows that reduction of the *p18* gene significantly enhanced high-grade PIN and carcinoma susceptibility in *Pten*$^{+/-}$ mice. (e) Increase of cell proliferation in *p18 Pten* double mutant prostatic epithelium. Eight-week-old tumor-free prostates from mice of different genotypes were stained with antibody recognizing phosphorylated histone H3. Positive nuclei were counted in 10 randomly chosen fields.

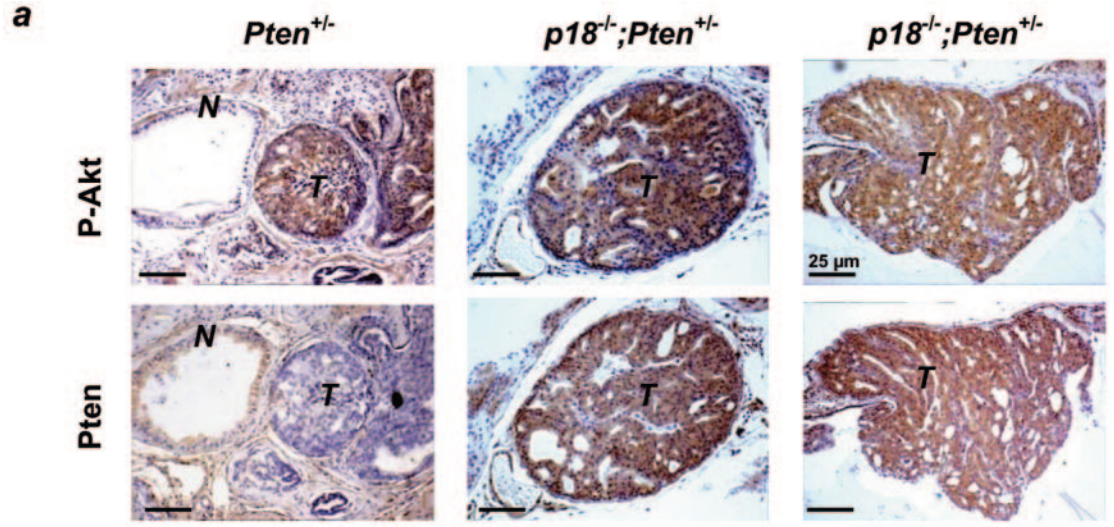

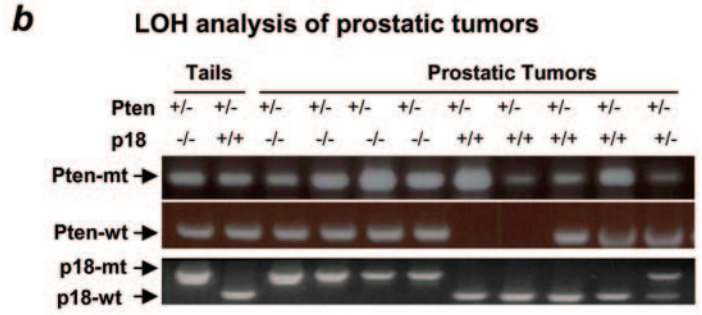

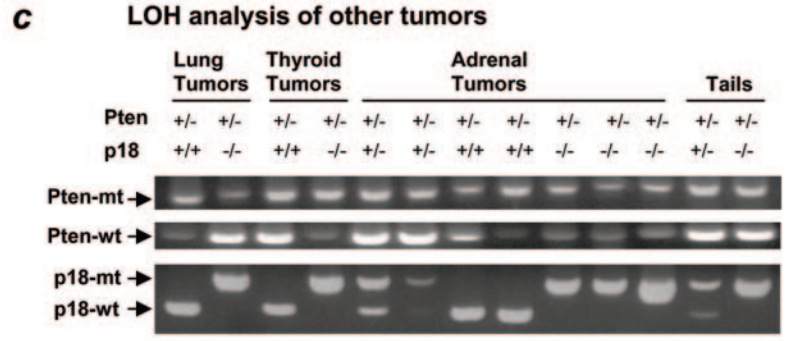

d

***Pten* and P-Akt expression status (Pten-/p-Akt+) in tumors by IHC**

Tumor	*p18*$^{-/-}$;*Pten*$^{+/-}$	*p18*$^{+/-}$;*Pten*$^{+/-}$	*Pten*$^{+/-}$
Pituitary	0/10	0/5	0/5
Thyroid	0/8	0/5	0/12
Adrenal	0/10	0/8	0/9
Prostate	2/13	3/9	9/11

e

LOH analysis of microdissected tumor DNA by PCR

Tumor	*p18*$^{-/-}$;*Pten*$^{+/-}$	*p18*$^{+/-}$;*Pten*$^{+/-}$	*Pten*$^{+/-}$
Pituitary	0/3	0/0	0/2
Thyroid	0/2	0/0	0/0
Adrenal	0/13	0/7	0/9
Prostate	0/15	0/9	5/12

FIG. 5. Loss of the remaining wild-type *Pten* allele is tissue-specific and is protected by p18 loss. (a) Serial sections of prostate tumors from *Pten*$^{+/-}$ and *p18*$^{-/-}$ *Pten*$^{+/-}$ mice were immunostained with activated Akt and PTEN. Note the strong p-Akt staining in the tumor (T) cells and very faint (negative) p-Akt staining in the normal (N) epithelium. In *Pten*$^{+/-}$ prostates, there is a mutually exclusive staining pattern between *Pten*

the epithelium. At 9 months of age, all of the $p18^{-/-}$ $Pten^{+/-}$ and 40% of $p18^{+/-}$ $Pten^{+/-}$ prostates displayed high-grade PIN lesions or carcinomas, respectively, while 20% of the $Pten^{+/-}$ prostates developed high-grade PIN. By 12 months of age, all of the $p18^{+/-}$ $Pten^{+/-}$ mice also displayed high-grade PIN or carcinoma, whereas half of the $Pten^{+/-}$ prostates remained free of high-grade PIN (Fig. 4b, c, and d).

To determine the cellular basis of the *p18-Pten* collaboration, we analyzed cellular proliferation and apoptosis in the prostates of different genotypes from 8-week-old tumor-free mutant mice. As determined by TUNEL assays, no significant difference in the rate of apoptosis was detected in the prostates of different genotypes at this age (data not shown). Immunostaining with an antibody to mitosis-specific phosphorylated histone H3 revealed an increase of cell proliferation in the $p18^{-/-}$ and $Pten^{+/-}$ prostatic epithelium (Fig. 4e). The mitotic index was further increased in both $p18^{+/-}$ $Pten^{+/-}$ and $p18^{-/-}$ $Pten^{+/-}$ double mutant prostatic epithelium over the $p18^{-/-}$ cells (Fig. 4e). These results suggest that, as in the case of pituitary tumor development, reduction of *Pten* activity, like *p18* loss, promoted cell proliferation.

***Pten* haploinsufficiency in tumor suppression is tissue specific.** Development of tumors from *Pten* heterozygotes offered an opportunity to address the issue of *Pten* haploinsufficiency in tumor suppression. We took two approaches to this end: IHC of PTEN and activated Akt, and LOH analysis of the remaining *Pten* wild-type alleles. *Pten* was expressed in normal epithelium but not in tumor cells in $Pten^{+/-}$ prostates (Fig. 5a). Consecutive sections of the same tumor were stained with an antibody to Ser^{473}-phosphorylated Akt and demonstrated a substantially higher expression of activated Akt in the tumor cells than in the normal epithelium (Fig. 5a). These results suggest that the remaining wild-type *Pten* allele was lost in the prostate tumor cells. As determined by IHC, PTEN protein expression was lost in 9 out of 11 prostate tumors from $Pten^{+/-}$ mice. In contrast, loss of PTEN protein expression was not detected in any tumors from the pituitary ($n = 5$), thyroid ($n = 12$), and adrenal glands ($n = 9$). Activated Akt was readily detected in all these tumors (Fig. 5a and d). These results indicate a tissue-specific haploinsufficiency of the *Pten* gene in tumor suppression.

Loss of the remaining wild-type *Pten* allele is protected by *p18* loss in prostate tumors. We next examined the *Pten* and phospho-Akt expression patterns in *p18-Pten* compound mice. Surprisingly, most $p18^{-/-}$ $Pten^{+/-}$ prostate tumor cells retained *Pten* expression and yet were positive for phospho-Akt (Fig. 5a and d). Only 2 out of 13 $p18^{-/-}$ $Pten^{+/-}$ and 3 out of 9 $p18^{+/-}$ $Pten^{+/-}$ prostate tumors lost *Pten* expression as determined by IHC. These results revealed that loss of the wild-type *Pten* allele in $p18^{-/-}$ $Pten^{+/-}$ mice is protected by *p18* loss. To further confirm this, we conducted laser capture microdissection and genomic PCR. DNA was extracted from the tumor tissues under the microscope, and PCR-based LOH analysis was performed. Five out of 12 prostate tumors from $Pten^{+/-}$ mice exhibited loss of the wild-type *Pten* allele and retention of the null allele, whereas none of the tumors derived from *p18 Pten* compound mutant mice ($n = 15$ for $p18^{-/-}$ $Pten^{+/-}$ and $n = 9$ for $p18^{+/-}$ $Pten^{+/-}$) showed loss of the wild-type *Pten* allele (Fig. 5b and e), further confirming that LOH is not required for tumor development in these compound mutant mice. In addition to prostate tumors, we also performed LOH analysis for tumors derived from pituitary, thyroid, and adrenal glands and found no LOH in those tumors from either *Pten* alone or *p18 Pten* compound mutant mice (Fig. 5c and e), suggesting that LOH occurs in a tissue-specific way in prostate tumor development. Taken together, our results demonstrated that loss of the wild-type *Pten* allele in $Pten^{+/-}$ mice is prostate specific and is protected by *p18* loss.

***p18* loss enhances $Pten^{+/-}$-induced Akt activation in vivo, and inactivation of the Rb pathway increases Akt activation in vitro.** To determine how *p18* loss accelerates tumor development in a *Pten* heterozygous background, we examined the expression levels and distribution of activated Akt in the prostates of different genotypes. Only a marginal accumulation of activated Akt was seen in the wild-type prostatic epithelium as well as in the $p18^{-/-}$ prostatic epithelium despite its hyperplastic appearance (Fig. 6a). A clear increase of Ser^{473}-phosphorylated Akt was evident in some of the PIN I and PIN II regions of the $Pten^{+/-}$ prostatic epithelium. As seen by the intensity of immunostaining, there was a substantial increase of activated Akt in most of the $p18^{-/-}$ $Pten^{+/-}$ cells from both low- and high-grade PIN (Fig. 6a). To confirm the synergistic activation of Akt by *Pten* reduction and *p18* loss, we dissected prostate tissues of different genotypes, prepared the total protein extract, and determined the level of both total and Ser^{473}-phosphorylated Akt by direct immunoblotting (Fig. 6b). The steady-state level of total Akt was similar between wild-type and mutant tissues of the four different genotypes. Ser^{473}-phosphorylated Akt was nearly undetectable in wild-type tissues or in either $p18^{+/-}$ or $p18^{-/-}$ prostate tissues but was easily detected in $Pten^{+/-}$ tissues and was further increased in $p18^{-/-}$ $Pten^{+/-}$ tissues. These results indicate that p18 negatively regulates Akt activation in a recessive manner to PTEN function.

Synergistic activation of Akt by *Pten* heterozygosity and *p18* loss led us to investigate whether interference of the Rb pathway similarly activates Akt in *Pten*-deficient human prostate cells. We selected two relatively well-characterized human

and p-Akt expression in the tumor cells and normal epithelium. In $p18^{-/-}$ $Pten^{+/-}$ prostates, most tumor cells retained *Pten* expression. (b) Presence of the wild-type *Pten* allele in prostate tumors of $p18^{-/-}$ $Pten^{+/-}$ and $p18^{+/-}$ $Pten^{+/-}$ mice and absence of the wild-type *Pten* allele in half of the prostate tumors of $Pten^{+/-}$ mice. DNA extracted from the microdissected samples of mice of different genotypes was amplified by PCR to detect wild-type (wt) and mutant (mt) alleles of *Pten* and *p18*, respectively. (c) Presence of the wild-type *Pten* allele in other tumors of $p18^{-/-}$ $Pten^{+/-}$, $p18^{-/-}$ $Pten^{+/-}$, and $Pten^{+/-}$ mice. DNA extracted from the microdissected samples of mice of different genotypes was amplified by PCR to detect *Pten* and *p18* alleles. (d) Summary of the expression pattern of *Pten* and p-Akt in different organ tumors from mutant mice. *Pten* and p-Akt expression levels were determined by IHC, and the results are shown as the number of *Pten*-negative samples divided by the number of p-Akt-positive samples, staining for the same tumor sample in consecutive sections. (e) Summary of LOH analysis of microdissected tumor samples by PCR. The results are shown as the number of LOH divided by the number of total samples examined.

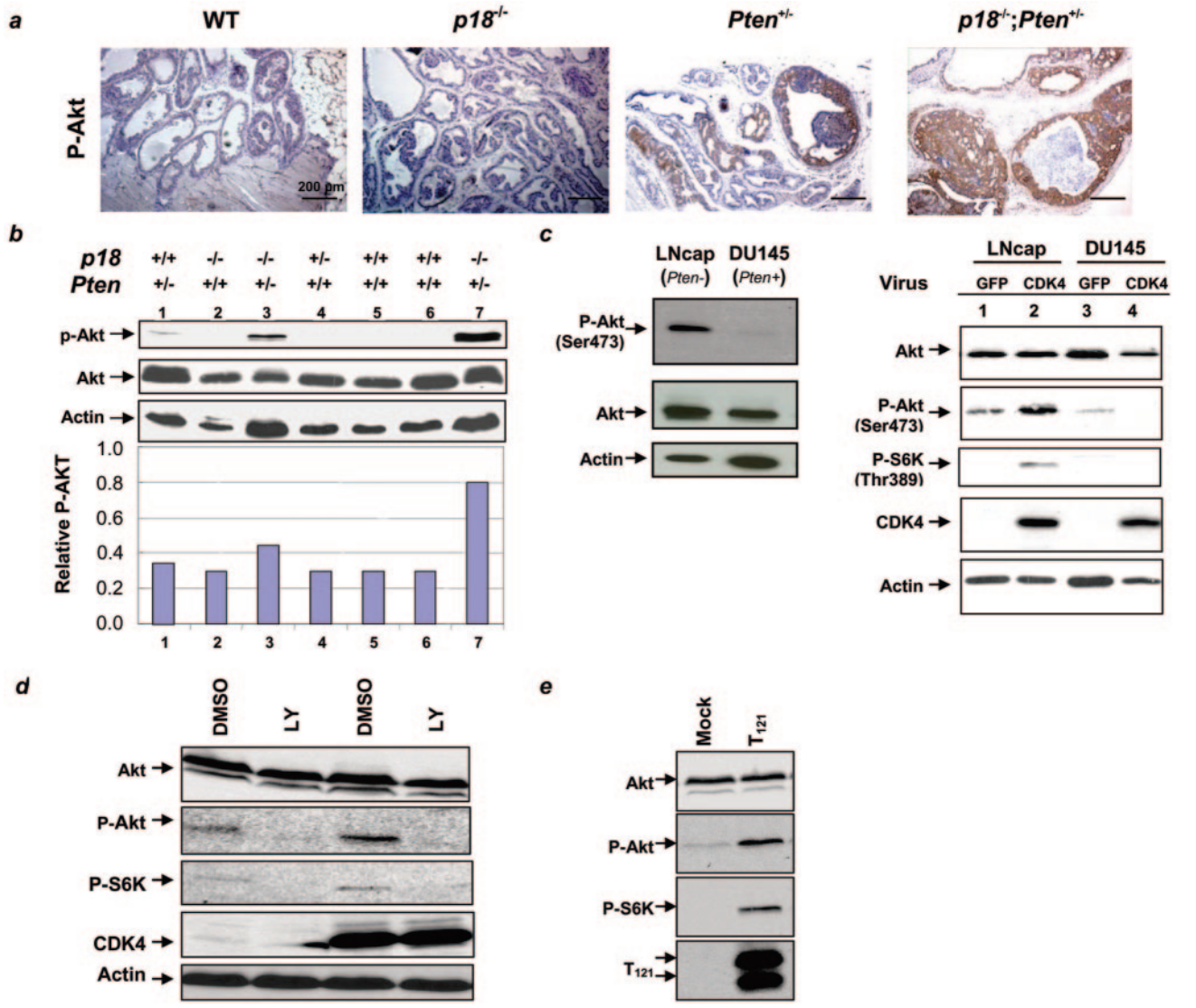

FIG. 6. Reduction or inactivation of the Rb pathway enhanced Akt activation in *Pten*$^{+/-}$ prostate cells. (a) Immunostaining for p-Akt of age-matched (9 months) prostates from mice of different genotypes. (b) Total cell lysates were prepared from the prostate tissues of mice of the indicated genotypes. Expression levels of total and Ser^{473}-phosphorylated Akt were determined by Western blot analysis. Expression of p-Akt was quantified by using NIH Image (version 1.33u), and the relative level of p-Akt to total Akt is shown. (c, left) Total cell lysates were prepared from the indicated cell lines. Expression patterns of total and Ser^{473}-phosphorylated Akt were determined by Western blot analysis. (Right) Overexpression CDK4 activated Akt. Cell lysates from the indicated cell lines infected with retroviruses expressing either CDK4 or GFP were prepared, and the steady-state levels of individual proteins were determined by Western blotting. (d) Inhibition of PI3K blocked Akt activation by CDK4. LNcap cells infected with either CDK4 or GFP were treated with LY294002 or dimethyl sulfoxide for 24 h, and then cell lysates were collected and analyzed by Western blotting. (e) Inactivation of Rb pathway-activated Akt and S6K. LNcap cells were transfected with pcDNA3-T_{121} or empty vector for 48 h, and cell lysates were collected and analyzed by Western blotting.

prostatic cancer cell lines: LNCaP, which expresses the wild-type *Rb* gene and is deficient for *Pten*, and DU145, which expresses wild-type *Pten* and a mutant *Rb* gene. While the steady-state level of total Akt is similar between these two cell lines, the levels of Ser^{473}- phosphorylated Akt are much higher in LNCaP cells than in DU145 cells (Fig. 6c), functionally confirming the status of *Pten*. The low level of activated Akt in DU145 cells is also consistent with the observation that a reduction of Rb pathway function is recessive to the *Pten* reduction in Akt activation.

To determine whether a decrease of Rb pathway activity would synergistically cause further Akt activation, we first transduced these cells with retroviruses expressing CDK4. Transduction of LNCaP cells with retroviruses expressing CDK4 did not cause any significant change of the steady-state level of Akt but increased the level of Ser^{473}-phosphorylated Akt as well as stimulated the Thr^{389} phosphorylation of S6K, a major downstream target of the Akt pathway (Fig. 6c). Treatment of CDK4-transduced LNCaP cells with LY294002, a selective inhibitor of phosphatidyl inositol 3-kinase (PI3K), inhibited CDK4-induced activation of both Akt and S6K (Fig. 6d), suggesting that activation of Akt by CDK4 is dependent on

PI3K-mediated Akt phosphorylation. This finding is consistent with the observation made in mouse prostate cells and tumors that stimulation of Akt phosphorylation by *p18* loss is recessive to *Pten* reduction and that similar CDK4 expression does not activate Akt in *Pten*-positive DU145 cells (Fig. 6c).

We then ectopically expressed in LNCaP and DU145 cells a fragment of T antigen containing the N-terminal 121 amino acids (T_{121}) that binds to all three pocket proteins, Rb, p107, and p130, and causes functional inactivation of the Rb pathway. LNCaP cells transfected with a plasmid expressing T_{121} expressed a similar level of Akt but had substantially increased Ser^{473}-phosphorylated Akt as well as Thr^{389}-phosphorylated S6K (Fig. 6e), providing further evidence that inactivation of the Rb pathway stimulates the PI3K-Akt pathway. Ectopically expressed T121 in DU145 cells did not activate Akt (data not shown).

DISCUSSION

In this paper, we provide evidence supporting a functional collaboration between the CDK inhibitor $p18^{Ink4c}$ and *Pten* in tumor suppression; both the rate and spectrum of tumor development in the compound mutant mice were substantially accelerated and expanded. Combined genetic, histological, cellular, and biochemical analyses led to four major findings: (i) that p18 and PTEN each have previously unrecognized functions in tumor suppression, such as p18's function in the prostate and anterior lobe of the pituitary and PTEN′s function in the pituitary, (ii) that the *p18-Pten* double mutant mice developed various stages of a prostate tumor phenotype in a gene dosage-dependent manner and with a high degree of penetrance, (iii) that *Pten* haploinsufficiency is tissue specific and is influenced by the status of other collaborating genes, such as *p18*, and (iv) that deletion of *p18* or inactivation of the Rb pathway increased activation of Akt that was recessive to the reduction of PTEN activity.

Human prostate cancer is characterized by the long latency between the appearance of precursor lesions (PIN) as early as in the twenties in men and the manifestation of clinically detectable carcinomas late in life (sixties or older). Historically, a major limitation toward this goal has been the lack of suitable animal models that faithfully recapitulate different stages of the prostate tumor progression, in large part because of anatomical differences and the differences in rate of tumor development between the mouse and human prostate (1). The *p18 Pten* double mutant mice developed various stages of prostate tumor phenotype in a gene dosage-dependent manner and with a high degree of penetrance. Importantly, prostate tumor phenotypes that developed in the *p18 Pten* double mutant mice occurred primarily in the dorsolateral prostate, a lobe analogous to the peripheral zone in the human prostate, where 80% of human prostate cancers arise. These findings present the *p18 Pten* mice, along with *p27 Pten* mice (7), as excellent models for studying mechanisms underlying the functional collaboration between different cellular pathways in suppression of prostate tumor development.

How widespread haploinsufficiency is among tumor suppressor genes is a topic of current interest (6, 26). Not only does this notion modify the concept that inactivating mutations in tumor suppressor genes are recessive, but it also bears a clinical implication: while both alleles of a haplosufficient tumor suppressor gene are inactivated in tumors, a haploinsufficient tumor suppressor gene usually retains at least one allele in tumors and thus represents a potential target of therapeutic intervention. The issue concerning the haploinsufficiency of *Pten* has been a subject of debate. While biallelic loss of *Pten* has been reported widely in human tumors, tumor-associated LOH of *Pten* in mice has thus far produced a different and more mixed pattern. The remaining wild-type *Pten* allele sustained allelic loss in most of the radiation-induced lymphomas derived from both $Pten^{+/-}$ single as well as $Pten^{+/-}$ $p53^{+/-}$ double heterozygotes (24) and in prostate tumors that developed in $Nkx3.1^{+/-}$ $Pten^{+/-}$ mice (16), but it was retained in a significant portion of prostate tumors that developed in $Pten^{+/-}$ TRAMP mice (19). We showed here that in $Pten^{+/-}$ mice *Pten* sustained a high frequency of allelic loss in prostate tumors but not in tumors of the pituitary, thyroid, and adrenal glands. Furthermore, we showed that the remaining *Pten* allele was lost in about half of prostate tumors that developed in $Pten^{+/-}$ mice but in none of the prostate tumors that developed in $p18^{-/-}$ $Pten^{+/-}$ or $p18^{+/-}$ $Pten^{+/-}$ double mutant mice. It is surprising that even loss of one allele of *p18* is sufficient to protect *Pten* loss. From these results, we suggest that the haploinsufficiency of *Pten*, and possibly other tumor suppressor genes, is both tissue specific and depends on genetic background.

In searching for the biochemical mechanism underlying the *p18-Pten* collaboration, we found that a reduction of the Rb pathway activity, either by the loss of *p18*, overexpression of *Cdk4*, or inactivation of Rb family proteins, activated Akt and its downstream target, S6K, in a manner that was genetically recessive to the function of PTEN. The detailed biochemical mechanisms by which the Rb pathway negatively regulates Akt remain to be determined but, likely, the Rb pathway acts upstream of PI3K, since the activation of Akt by CDK4 overexpression can be blocked by the PI3K inhibitor (Fig. 6d). We speculate that one or more E2F target genes, such as the adaptor protein Grb2-associated binder 2 (5), may function upstream of PI3K to regulate the Akt-dependent cell growth pathway. It has long been recognized that cell cycle (cell doubling) and cell growth (increase of cell mass) must be coordinately regulated. Early studies from yeast cells have established that when cell growth is blocked by nutrient deprivation or by inactivating key biosynthetic genes, the cell cycle can no longer proceed (15), indicating a control of cell cycle, or G_1-to-S transition, by the growth status. Our finding that a reduction of PTEN resulted in an increase of cell proliferation supports this notion (Fig. 2c and 4e). The finding that a disruption of the Rb pathway stimulates Akt-mediated cell growth suggests a cross talk between the cell growth and cell cycle pathways. We suggest that stimulation of the cell growth pathway by events controlling the G_1-to-S transition serves to ensure sustained growth through the remainder of the cell cycle. As such, a simultaneous stimulation of both pathways, such as created here by the mutation in one negative regulator from each pathway or mutations targeting both pathways, as observed in human cancers, would prove more advantageous, if not necessary, for cell proliferation and tumor development.

ACKNOWLEDGMENTS

We thank Jerrold M. Ward and Chad McCall for reading the manuscript, Virginia Godfrey for helping with histological examination, Matthew Smith for helping with mouse genotyping, necropsy, immunohistochemistry, laser microdissection, and production of the histologic sections, and Yizhou He for helping with figure preparation.

F.B. is supported in part by a U.S. Department of Defense Career Postdoctoral fellowship (D.A.). This study was supported by NIH grant CA68377 and Department of Defense Prostate Cancer Research grant PC040835 to Y.X.

REFERENCES

1. **Abate-Shen, C., and M. M. Shen.** 2000. Molecular genetics of prostate cancer. Genes Dev. **14:**2410–2434.
2. **Bai, F., X. H. Pei, V. L. Godfrey, and Y. Xiong.** 2003. Haploinsufficiency of $p18^{INK4c}$ sensitizes mice to carcinogen-induced tumorigenesis. Mol. Cell. Biol. **23:**1269–1277.
3. **Cantley, L. C.** 2002. The phosphoinositide 3-kinase pathway. Science **296:**1655–1657.
4. **Cantley, L. C., and B. G. Neel.** 1999. New insights into tumor suppression: PTEN suppresses tumor formation by restraining the phosphoinositide 3-kinase/AKT pathway. Proc. Natl. Acad. Sci. USA **96:**4240–4245.
5. **Chaussepied, M., and D. Ginsberg.** 2004. Transcriptional regulation of AKT activation by E2F. Mol. Cell **16:**831–837.
6. **Cook, W. D., and B. J. McCaw.** 2000. Accommodating haploinsufficient tumor suppressor genes in Knudson's model. Oncogene **19:**3434–3438.
7. **Di Cristofano, A., M. De Acetis, A. Koff, C. Cordon-Cardo, and P. P. Pandolfi.** 2001. Pten and $p27^{KIP1}$ cooperate in prostate cancer tumor suppression in the mouse. Nat. Genet. **27:**222–224.
8. **Di Cristofano, A., P. Kotsi, Y. F. Peng, C. Cordon-Cardo, K. B. Elkon, and P. P. Pandolfi.** 1999. Impaired Fas response and autoimmunity in $Pten^{+/-}$ mice. Science **285:**2122–2125.
9. **Di Cristofano, A., B. Pesce, C. Cordon-Cardo, and P. P. Pandolfi.** 1998. Pten is essential for embryonic development and tumor suppression. Nat. Genet. **19:**348–355.
10. **Ezzat, S., S. L. Asa, W. T. Couldwell, C. E. Barr, W. E. Dodge, M. L. Vance, and I. E. McCutcheon.** 2004. The prevalence of pituitary adenomas: a systematic review. Cancer **101:**613–619.
11. **Franklin, D. S., V. L. Godfrey, H. Lee, G. I. Kovalev, R. Schoonhoven, S. Chen-Kiang, L. Su, and Y. Xiong.** 1998. CDK inhibitors $p18^{INK4c}$ and $p27^{KIP1}$ mediate two separate pathways to collaboratively suppress pituitary tumorigenesis. Genes Dev. **12:**2899–2911.
12. **Franklin, D. S., V. L. Godfrey, D. A. O'Brien, C. Deng, and Y. Xiong.** 2000. Functional collaboration between different cyclin-dependent kinase inhibitors suppresses tumor growth with distinct tissue specificity. Mol. Cell. Biol. **20:**6147–6158.
13. **Hanahan, D., and R. A. Weinberg.** 2000. The hallmarks of cancer. Cell **100:**57–70.
14. **Jacks, T., A. Fazeli, E. M. Schmitt, R. T. Bronson, M. A. Goodell, and R. A. Weinberg.** 1992. Effects of an Rb mutation in the mouse. Nature **359:**295–300.
15. **Johnston, G. C., J. R. Pringle, and L. H. Hartwell.** 1977. Coordination of growth with cell division in the yeast Saccharomyces cerevisiae. Exp. Cell Res. **105:**79–98.
16. **Kim, M. J., R. D. Cardiff, N. Desai, W. A. Banach-Petrosky, R. Parsons, M. M. Shen, and C. Abate-Shen.** 2002. Cooperativity of Nkx3.1 and Pten loss of function in a mouse model of prostate carcinogenesis. Proc. Natl. Acad. Sci. USA **99:**2884–2889.
17. **Knudson, A. G.** 1971. Mutation and cancer: statistical study of retinoblastoma. Proc. Natl. Acad. Sci. USA **68:**820–823.
18. **Krimpenfort, P., K. C. Quon, W. J. Mooi, A. Loonstra, and A. Berns.** 2001. Loss of $p16^{Ink4a}$ confers susceptibility to metastatic melanoma in mice. Nature **413:**83–86.
19. **Kwabi-Addo, B., D. Giri, K. Schmidt, K. Podsypanina, R. Parsons, N. Greenberg, and M. Ittmann.** 2001. Haploinsufficiency of the Pten tumor suppressor gene promotes prostate cancer progression. Proc. Natl. Acad. Sci. USA **98:**11563–11568.
20. **Latres, E., M. Malumbres, R. Sotillo, J. Martin, S. Ortega, J. Martin-Caballero, J. M. Flores, C. Cordon-Cardo, and M. Barbacid.** 2000. Limited overlapping roles of $p15^{INK4b}$ and $p18^{INK4c}$ cell cycle inhibitors in proliferation and tumorigenesis. EMBO J. **19:**3496–3506.
21. **Lee, Y.-H. P., C.-Y. Chang, N. Hu, Y.-C. J. Wang, C.-C. Lai, K. Herrup, W.-H. Lee, and A. Bradley.** 1992. Mice deficient for Rb are nonviable and show defects in neurogenesis and haematopoiesis. Nature **359:**288–294.
22. **Maandag, E. C., M. Van Der Valk, M. Vlaar, C. Feltkamp, J. O'Brien, M. Van Roon, N. Van Der Lugt, A. Berns, and H. Te Riele.** 1994. Developmental rescue of an embryonic-lethal mutation in the retinoblastoma gene in chimeric mice. EMBO J. **13:**4260–4268.
23. **Maehama, T., and J. E. Dixon.** 1998. The tumor suppressor, PTEN/MMAC1, dephosphorylates the lipid second messenger, phosphatidylinositol 3,4,5-triphosphate. J. Biol. Chem. **273:**13375–13378.
24. **Mao, J. H., D. Wu, J. Perez-Losada, H. Nagase, R. DelRosario, and A. Balmain.** 2003. Genetic interactions between Pten and p53 in radiation-induced lymphoma development. Oncogene **22:**8379–8385.
25. **Podsypanina, K.** 1999. Mutation of Pten/Mmac1 in mice causes neoplasia in multiple organ systems. Proc. Natl. Acad. Sci. USA **96:**1563–1568.
26. **Quon, K. C., and A. Berns.** 2001. Haplo-insufficiency? Let me count the ways. Genes Dev. **15:**2917–2921.
27. **Sharpless, N. E., N. Bardeesy, K. H. Lee, D. Carrasco, D. H. Castrillon, A. J. Aguirre, E. A. Wu, J. W. Horner, and R. A. DePinho.** 2001. Loss of $p16^{Ink4a}$ with retention of $p19^{Arf}$ predisposes mice to tumorigenesis. Nature **413:**86–91.
28. **Sherr, C. J.** 1996. Cancer cell cycle. Science **274:**1672–1677.
29. **Sotillo, R., P. Dubus, J. Martin, E. de La Cueva, S. Ortega, M. Malumbres, and M. Barbacid.** 2001. Wide spectrum of tumors in knock-in mice carrying a Cdk4 protein insensitive to INK4 inhibitors. EMBO J. **20:**6637–6647.
30. **Stambolic, V., M. S. Tsao, D. Macpherson, A. Suzuki, W. B. Chapman, and T. W. Mak.** 2000. High incidence of breast and endometrial neoplasia resembling human Cowden syndrome in $pten^{+/-}$ mice. Cancer Res. **60:**3605–3611.
31. **Wang, S., J. Gao, Q. Lei, N. Rozengurt, C. Pritchard, J. Jiao, G. V. Thomas, G. Li, P. Roy-Burman, P. S. Nelson, X. Liu, and H. Wu.** 2003. Prostate-specific deletion of the murine Pten tumor suppressor gene leads to metastatic prostate cancer. Cancer Cell **4:**209–221.
32. **Weinberg, R. A.** 1995. The retinoblastoma protein and cell cycle control. Cell **81:**323–330.
33. **Williams, B. O., L. Remington, D. M. Albert, S. Mukai, R. T. Bronson, and T. Jacks.** 1994. Cooperative tumorigenic effects of germline mutations in *Rb* and *p53*. Nat. Genet. **7:**480–484.